

## Effects of disorder in pattern formation

Walter Zimmermann

*Institut für Festkörperforschung, Forschungszentrum Jülich, D-52425 Jülich, Federal Republic of Germany*

Markus Seesselberg and Francesco Petruccione

*Fakultät für Physik, Albert-Ludwigs-Universität, D-79104 Freiburg im Breisgau, Federal Republic of Germany*

(Received 18 September 1992)

The interplay between localization and nonlinearity is investigated for a modified Swift-Hohenberg equation. We introduced a spatially stochastic contribution  $\eta\xi(x)$  in the control parameter that mimics, for instance, the essential effects of irregularities at the top and bottom plate in Rayleigh-Bénard-convection experiments. Near the threshold where the trivial solution  $u \equiv 0$  becomes unstable, this randomness leads to localized solutions. Furthermore, the threshold value of the spatially averaged control parameter is reduced by the disorder  $\eta\xi(x)$ . The interaction between localization and nonlinearity leads to a characteristic change of the nonlinear bifurcation behavior. When ramping the control parameter in time, the disorder leads to an earlier onset and to a less steep temporal evolution of the pattern. This static and dynamic nonlinear behavior has similarities with recent measurements on Rayleigh-Bénard convection.

PACS number(s): 47.20.Ky, 71.55.-i

In the past decades there has been enormous progress in identifying the essential role that nonlinearity plays in physical systems [1]. During the same period, similar progress occurred in understanding linear effects of disorder in solid-state [2,3] or in classical waves [4,5]. Significantly, these two developments have occurred rather independently, whereas in real systems both coexist presumably often. Nonlinear properties play an essential role in pattern-forming systems such as Rayleigh-Bénard (thermal) convection, Taylor-Couette flow, and electroconvection in nematic liquid crystals or solidification fronts [1]. Here we investigate the influence of frozen disorder in the control parameter of a modified Swift-Hohenberg (SH) equation [6]. We find a reduction of the threshold for pattern formation, localized solutions, and a general signature of the interaction between localization and the nonlinearity.

The container boundaries of the mentioned pattern-forming systems usually have a finite roughness. Often this is small compared to the container extensions and the related effects are beyond the experimental resolution. For such situations the usual assumption of ideal flat container boundaries is a good approximation. However, recent experiments are designed with smaller container extensions and the detection sensitivity is also under continuous improvement. Both tendencies make it more likely that in experiments roughness effects possibly arise, which will be puzzling within an analysis based on ideal flat container boundaries. It is therefore important to know the container dimensions and parameter ranges where the typical roughness effects occur. Thermal convection, for instance, plays an important role for many processes in geophysics and meteorology and several of them are investigated in the laboratory, however, with the fluids or gases in containers having rather (ideal) flat boundaries. To extrapolate back to the outdoor systems

without well-defined boundaries, it is important to know about the robustness of phenomena under laboratory conditions against irregularities. In hydrodynamic systems with rough container boundaries or macroscopic porosity [7] new disorder phenomena may arise.

Motivated by that we analyze in a first step a simple pattern-forming system with a random contribution in the control parameter, a modified version of the Swift-Hohenberg equation. The SH equation in its original version [6] approximates Rayleigh-Bénard convection for large Prandtl numbers reasonably near the onset of convection rolls. In a dimensionless version the modified SH equation is

$$\partial_t u = \{\epsilon + \eta\xi(x) - (1 + \partial_x^2)^2\}u - u^3 + \sigma f(x, t) \quad (1)$$

which has in physical units of Rayleigh-Bénard convection the form

$$\tau_0 \partial_t u' = \{\epsilon' + \eta'\xi(x') - \frac{\xi_0^2}{4q_c^2}(q_c^2 + \partial_x'^2)^2\}u' - hu'^3 + \sigma' f(x, t) \quad (2)$$

with  $x = q_c x'$ ,  $t = \xi_0^2 q_c^2 / (4\tau_0) t'$ ,  $u = \sqrt{4h / (\xi_0^2 q_c^2)} u'$ ,  $\sigma = 4 / (\xi_0^2 q_c^2) \sigma'$ ,  $\epsilon = \epsilon' 4 / \xi_0^2 q_c^2$ , and  $\eta = \eta' 4 / \xi_0^2 q_c^2$ . The constants  $\tau_0 = 0.0552$ ,  $\xi_0/d = 0.3848$  are the characteristic time and length scales,  $q_c d = 3.116$  is the critical wave number, and  $h = 0.699$  is the coefficient of the nonlinear term. The values of the constants are taken from [8,9] where they are given for  $\eta = 0$ .  $\epsilon$  measures the distance from the bifurcation point and  $x$  is in the Rayleigh-Bénard system the spatial coordinate across the convection rolls.  $\epsilon'$  is the reduced Rayleigh number

$$\epsilon' = \frac{R - R_c}{R_c} \quad (3)$$

The Rayleigh number  $R$  itself [8],

$$R = \frac{\rho_0 \alpha g \Delta T d^3}{\kappa \nu}, \quad (4)$$

characterizes the external stress in Rayleigh-Bénard convection, wherein  $\rho_0$  is the mass density,  $\alpha$  the thermal expansion coefficient of the respective fluid,  $g$  the gravitation constant,  $d$  the thickness of the fluid layer,  $\kappa$  the thermal diffusivity,  $\nu$  the kinematic viscosity, and  $\Delta T$  the temperature difference between the upper and bottom plates. In the Rayleigh-Bénard cell the convection starts when the temperature difference becomes larger than a critical value  $\Delta T_c$ . This defines due to Eq. (3) the critical Rayleigh number  $R_c = 1704$ , which is a universal number independent of the used fluid and the layer thickness.

The random contribution  $\eta \xi(x)$  introduced in the SH equation may be considered as an *ad hoc* generalization. In the context of Rayleigh-Bénard convection the randomness mimics main effects of irregularities in the confining top and bottom container boundary also causing fluctuations in the thickness of the fluid layer  $d$ . Taking  $d_0$  as the mean value we choose for the fluctuating thickness the following expression:

$$d = d_0 \left[ 1 + \frac{\eta'}{3} \xi(x) \right]. \quad (5)$$

With the definition  $R_c = R(d = d_0)$  it is easy to see from Eq. (4) how the thickness fluctuations transform into a random component of the Rayleigh number  $R$ . The control parameter in the rescaled equation (1) has then the explicit form:  $\epsilon + \eta \xi(x)$ .

Since we do not know the detailed form of the irregularities at the confining boundaries we choose  $\xi(x)$  as an exponentially correlated Ornstein-Uhlenbeck process in space [9] with vanishing spatial mean value and the correlation length  $l$ :

$$\langle \xi(x) \rangle = 0, \quad \langle \xi(x) \xi(x'') \rangle = \exp(-|x - x''|/l). \quad (6)$$

Throughout this work we take  $l = \pi = \lambda_c/2$ , where  $\lambda_c$  is the second length scale determined by the convection roll diameter at the critical Rayleigh number  $R_c$  [8]. Additionally we investigate Eq. (1) for a finite, experimentally reasonable length  $L = 20\lambda_c$ . In this case large and for many pattern-forming systems unphysical fluctuations [ $\eta \xi(x) \sim d_0$ ] have a small weight and the ensemble and spatial average  $\langle \langle |\eta \xi_i(x)| \rangle \rangle / d_0$  can be restricted to small values. A typical realization of the stochastic process  $\xi(x)$  is shown in Fig. 1(a). The forcing term  $f(x, t)$  in Eq. (1) is supposed to mimic thermal fluctuations and we choose it as an uncorrelated Gaussian random field, which satisfies

$$\begin{aligned} \langle f(x, t) \rangle &= 0, \\ \langle f(x, t) f(x'', t'') \rangle &= \delta(x - x'') \delta(t - t''). \end{aligned} \quad (7)$$

We solve Eq. (1) numerically for periodic boundary conditions:  $u(0) = u(L)$ . The numerical treatment of stochastic partial differential equations is found in [10]. The discretized version of the full SH equation is solved via

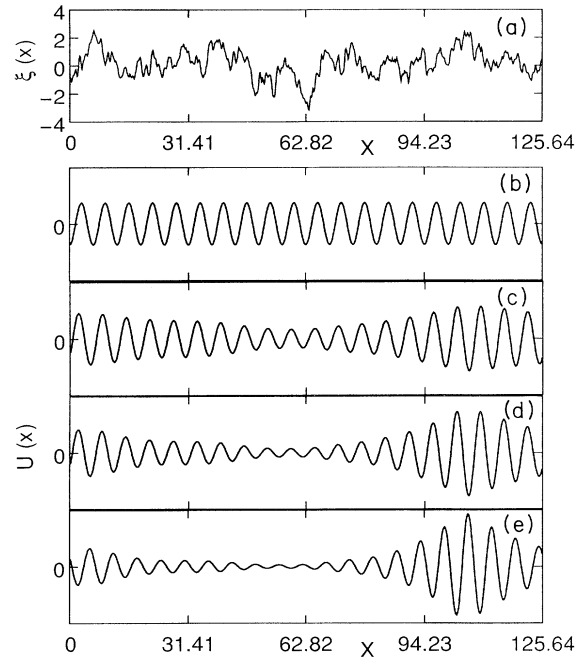


FIG. 1. In (a) we show a typical realization of  $\xi(x)$  and in (b)–(d) the eigensolutions to the respective largest eigenvalues of the linear part of the SH equation (1) for different values of the perturbation strength  $\eta$ . (b)  $\eta = 0.0$ , (c)  $\eta = 0.005$ , (d)  $\eta = 0.01$ , and (e)  $\eta = 0.015$ .

standard implicit-difference schemes (Cranck-Nicholson) and for calculating stationary solutions without additive noise ( $\sigma = 0$ ) Newton schemes are used.

The convective heat current is the measurable quantity which can be compared after rescaling with the dimensionless convective heat current [11,12]

$$J = \frac{1}{L} \int_0^L dx [u(x, t)]^2, \quad (8)$$

where  $u(x)$  is a solution of the SH equation (1).

At first we discuss the effects of  $\eta \xi(x)$  on the linear part of Eq. (1) and we neglect the cubic term as well as thermal fluctuations ( $\sigma = 0$ ). The trivial solution  $u \equiv 0$  loses its stability without disorder ( $\eta = 0$ ) at positive values of  $\epsilon > \epsilon_c = 0$ . With disorder ( $\eta \neq 0$ ) the control parameter  $\epsilon + \eta \xi(x)$  becomes in some regions earlier overcritical and the trivial solution  $u = 0$  loses its stability already at slightly negative values of  $\epsilon$ . The actual values of  $\epsilon_c < 0$  depend on the system length  $L$  and the correlation length  $l$  as well as on the realization of the stochastic process  $\xi(x)$ . We evaluate the ensemble average of the critical value  $\epsilon_c(\eta) = \langle \epsilon_c(\eta, i) \rangle$  over 600 realizations of the stochastic process  $\xi(x)$  for different values of  $\eta$ . As a result we obtained the power law  $\epsilon_c(\eta) \sim -\eta^\alpha$ ,  $\alpha = 1.46$ . Analytically we find for the uncorrelated disorder ( $l = 0$ )  $\epsilon_c \propto -\eta^{4/3}$  and for a finite correlation length  $l$  a more complex transcendental expression for  $\epsilon_c$ , interpolating between  $\epsilon_c \propto -\eta^{4/3}$  for  $l \ll 1$  and the simple linear shift of  $\epsilon_c \propto -\eta$  for  $l \gg 1$  [13]. (Recently Pomeau received qualitatively similar results by a different analysis of the linear part of our model in Eq. (1) [14].)

At  $\eta=0$  the eigenfunctions of the linear part  $\epsilon + \eta\xi(x) - (1 + \partial_x^2)^2$  of Eq. (1) are simple harmonic functions such as  $\sin(qx)$  or  $\cos(qx)$  while its spatial dependence becomes for increasing values of  $\eta$  more and more localized in those regions where  $\epsilon + \eta\xi(x)$  takes its largest values. For a typical realization of  $\xi(x)$  shown in Fig. 1(a) and for four different values of  $\eta$  we have plotted in Figs. 1(b)–1(e) the eigenfunctions of the linear operator in Eq. (1) corresponding to the largest eigenvalue. The eigenfunctions with the next largest eigenvalues show a similar localization behavior, but their “pulses” are located in different parts of the interval  $(0, L)$  as shown in Fig. 2 for  $\eta=0.02$  and the same random process as in Fig. 1(a). For very small and large values of the correlation length  $l$  the localization of the eigenfunctions becomes weaker, because the randomness averages out on the scale of one period for small  $l$  and at very large values for  $l$  very wide regions pass the threshold simultaneously. The localization behavior has similarities with the Anderson localization in solid-state physics [3] and has important consequences on the nonlinear bifurcation behavior discussed below.

In the unperturbed case ( $\eta=0$ ) all the eigensolutions corresponding to different eigenvalues of the linear operator in Eq. (1) are harmonic functions. The nonlinear interaction between those is competitive and as a consequence the stationary solution of the nonlinear SH equation is essentially the harmonic function. For  $\eta=0$  the cubic nonlinearity leads to the proportionality  $J \sim \epsilon$ . In the following we explain that for  $\eta \neq 0$  the functional dependence of  $J(\epsilon)$  is more complex.

The disorder induced shift of the threshold to  $\langle \epsilon_c(\eta, i) \rangle < 0$  and the localization of the eigenfunctions lead to a characteristic change of the curve  $J(\epsilon)$ . To demonstrate this, we generated 30 realizations of the stochastic process  $\xi_i(x)$ ,  $i=1, \dots, 30$ , and evaluated the corresponding critical values of the control parameter  $\epsilon_c(\eta, i)$  for different values of  $\eta$ . Next we calculated the

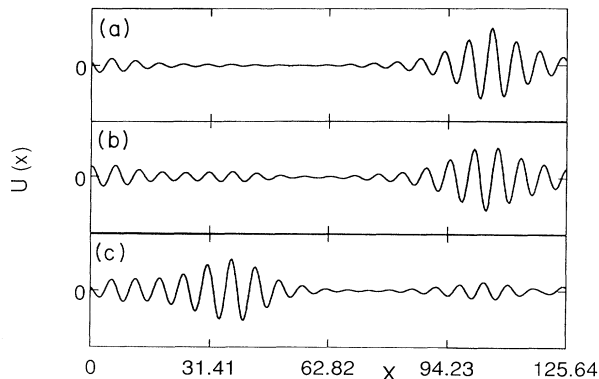


FIG. 2. The eigenfunctions corresponding to the largest three eigenvalues of the linear part of Eq. (1) are shown for the same  $\xi(x)$  and as given in Fig. 1(a) and for  $\eta=0.02$ . The two rather similar eigenfunctions in (a) and (b) developed out of the symmetric  $\cos$  and the antisymmetric  $\sin$  of the unperturbed problem ( $\eta=0$ ). In the unperturbed case their eigenvalues are degenerated, however not in our case. The corresponding eigenfunction to (c), similar as (b) to (a), exists also.

stationary convective heat current  $J_i(\epsilon - \epsilon_c(\eta, i))$  and then the expectation value

$$\langle J(\epsilon, \eta) \rangle = \frac{1}{30} \sum_{i=1}^{30} J_i(\epsilon - \epsilon_c(\eta, i)), \quad (9)$$

which we have plotted in Fig. 3. The slope of  $\langle J(\epsilon, \eta) \rangle$  increases now for increasing values of  $\epsilon$  and converges finally to the constant slope for  $\eta=0$ . For finite values of  $\eta$  immediately above the threshold  $\epsilon_c(\eta, i)$ , where the first eigenvalue is already positive, however, the second eigenvalue still negative,  $J_i(\epsilon - \epsilon_c(\eta, i))$  is, due to the cubic nonlinearity, a straight line. When the second eigenvalue also becomes positive and the overlap between the two respective eigenfunctions is still small, then the eigenfunctions at finite amplitudes interact only slightly via the nonlinearity. Thus the second eigenfunction at a finite amplitude contributes additively to  $J_i(\epsilon - \epsilon_c(\eta, i))$  and increases its slope. With increasing  $\epsilon$  the eigenvalues of further eigenfunctions become positive and therefore the interaction between those is increasing. This finally leads for  $[|\eta\xi(x)| \ll \epsilon]$  to solutions again resembling a harmonic function. The slope of  $J_i(\epsilon - \epsilon_c(\eta, i))$  and therefore also of  $\langle J(\epsilon, \eta) \rangle$  changes just in the range, where the overlap between the first eigenfunctions increases. That means the influence of the randomness has its largest effect near the onset of the pattern  $u(x)$ .

This transition behavior becomes even more pronounced when one considers instead of  $\langle J(\epsilon, \eta) \rangle$  another often used quantity  $\mathcal{C} = \sqrt{\langle J(\epsilon, \eta) \rangle}$ . At  $\eta=0$  the curvature  $d^2\mathcal{C}/d\epsilon^2$  is negative immediately above threshold, however, at finite values for  $\eta$  this curvature changes its sign with increasing  $\epsilon$  in the transition range. The curvature is negative immediately above threshold and at larger values of  $\epsilon$  and positive in the transition range.

So far we considered the convective heat current  $J$  only for stationary solutions  $u(x)$ . In Fig. 4 we show the temporal evolution of  $\langle J(\epsilon(t)) \rangle = \frac{1}{30} \sum_{i=1}^{30} J_i(\epsilon(t) - \epsilon_c(\eta, i))$  for the case of a ramped control parameter  $\epsilon(t) = -0.15 + 0.00278t$ . The different curves corre-

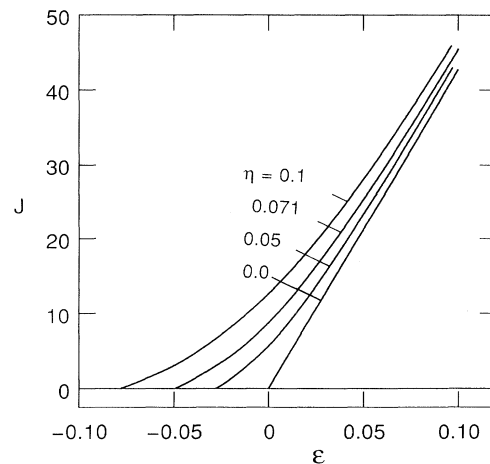


FIG. 3. For different strengths  $\eta=0.0, 0.05, 0.071$ , and  $0.10$  of the random part  $\eta\xi(x)$  in the control parameter the averaged convection heat current  $\langle J(\epsilon) \rangle$  as defined in Eq. (9) is shown.

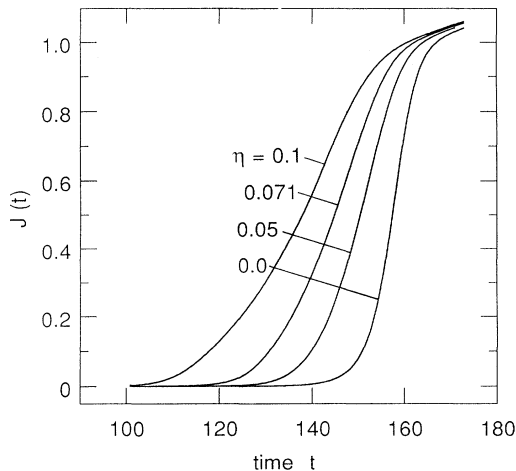


FIG. 4. The averaged convection heat current  $\langle J(\epsilon) \rangle$  is plotted as a function of time in the case of a ramped control parameter  $\epsilon(t) = -0.15 + 0.00278t$ . The curves correspond to different values  $\eta = 0, 0.050, 0.071, 0.10$  and the additive noise strength was fixed at  $\sigma = 10^{-7}$ .

spond to different values of  $\eta = 0, 0.050, 0.071, 0.100$  and the additive noise strength was fixed at  $\sigma = 10^{-7}$ . These curves show two remarkable features: the earlier onset of the convective heat current and its decreasing slope of  $J(t)$  for increasing values of  $\eta$ .

Now we give a quantitative estimate about the relations between the fluctuations in the fluid layer thickness and the random contribution  $\eta\xi(x)$ . The standard deviation of the stochastic process  $\xi(x)$  is 1 according to Eq. (6). The values of  $\eta$  used in Figs. 3 and 4 are between 0.1 and 0.05 ( $\eta' = 0.036$  or  $0.018$ ) corresponding via Eq. (5) to the typical fluctuations of the layer thickness of about 1.2% or 0.6%. For comparison an upper limit for the fluctuations of the layer thickness is 0.5% in the experiments of Meyer, Ahlers, and Cannell [12].

By comparing the curves in Figs. 3 and 4 with the measurements in Ref. [12], we find the following remarkable similarities. The slope of the fit curve to the measured stationary convective heat current in Fig. 5 of Ref. [12] is increasing with  $\epsilon$ , similar as the slope of the curves in Fig. 3 at finite values of  $\eta$ . For a ramped control parameter the onset of  $J(t)$  in the experiment [12] was much earlier than expected from calculations on the SH equation with additive noise  $\sigma f(x, t)$  [12,15] and the noise strength  $\sigma$  calculated from the Navier-Stokes equations [9,16]. To obtain an onset time as early as in the experiment, a noise strength  $\sigma$  was necessary, which is two orders of magnitude larger than calculated [12,15]. For comparison in

our calculations at  $\eta = 0.071$  [ $\equiv (d - d_0)/d_0 \sim 0.9\%$ ] we also obtained an onset time, which can only be reproduced with  $\eta = 0.0$ , when the additive noise strength  $\sigma$  is chosen two orders of magnitude larger than in the case  $\eta = 0.071$ . The slopes of the curves in Fig. 4 for finite values of  $\eta$  as well as the curve of the measured heat current in the ramping experiments (see, for instance, Figs. 12 and 13 in Ref. [12]) are less steep during the transition from  $J \ll 1$  to its nonlinear saturation value than for  $\eta = 0$ .

In conclusion we have shown in Fig. 3 the consequences of the interaction between localization and nonlinearity and their possible experimental relevance. Whenever measurements show for instance a deviation from the expected supercritical bifurcation as in Fig. 3 one must be careful to interpret it as an imperfect bifurcation in the classical definition: It may still be a sharp bifurcation, however, shifted to lower values of the control parameter as in our case and a consequence of the roughness at the container boundaries. Figure 4 shows that the roughness could be the reason for an unexpected early onset of the heat current in the experiments. Presumably these effects are even more pronounced in a two-dimensional SH equation and therefore quantitatively even narrower in the quasi-two-dimensional experimental situation [12].

The shown threshold shifts and the interplay of localization and nonlinearity is rather general and we expect that it applies to other systems with spatially distributed disorder as well. Thereby we think of special physical systems such as high-temperature superconductors and convection in porous media [7], as well as of more general types of bifurcations, such as Hopf, codimension-2, and subcritical bifurcations. If one derives the SH equation in consideration of the roughness of the container boundaries in a Rayleigh-Bénard experiment more systematically, then besides the term  $\eta\xi(x)$  discussed here, a further term proportional to  $\hat{\xi}(x)u^2$  or local drift terms  $\hat{\xi}(x)\partial_x u$  occur. These additional terms modify the discussed effects slightly [13]. However, when such local drift effects dominate the ones discussed here, as it is presumably the case in electroconvection experiments, then very interesting disorder induced dynamical frustration effects arise [13]. One can easily imagine that similar disorder terms will influence the stability properties of the nonlinear solution (e.g., Eckhaus stability), front propagation, etc., which will be investigated in forthcoming works.

We thank G. Eilenberger, K. H. Fischer, J. Honerkamp, H. Müller-Krumbhaar, and W. Renz for useful hints.

[1] For numerous examples and references see, for instance, *Cellular Structures in Instabilities*, edited by J. E. Wesfreid and S. Zaleski (Springer, New York, 1984); *Propagation in Systems Far from Equilibrium*, edited by J. E. Wesfreid et al. (Springer, Berlin, 1988); *Nonlinear Evolutions of Spatio-temporal Structures in Dissipative Continuous Sys-*

*tems*, edited by F. H. Busse and L. Kramer (Plenum, New York, 1990); *Nonlinear Science: The Next Decade*, special issue of *Physica D* **51** (1991).

[2] P. A. Lee and T. V. Ramakrishnan, *Rev. Mod. Phys.* **57**, 287 (1985).

[3] For an overview, see *Chance and Matter*, edited by J.

- Souletie, J. Vannimenus, and R. Stora (Elsevier, Amsterdam, 1987).
- [4] P. Devillard, F. Dunlop, and B. Soulliard, *J. Fluid. Mech.* **186**, 521 (1988); M. Belzons, E. Guazelli, and O. Parodi, *ibid.* **186**, 539 (1988).
- [5] A. S. Mikhailov, *Phys. Rep.* **184**, 307 (1989).
- [6] J. Swift and P. C. Hohenberg, *Phys. Rev. A* **15**, 319 (1977).
- [7] D. A. Nield and A. Bejan, *Convection in Porous Media* (Springer, Berlin, 1992); L. Howle, R. P. Behringer, and J. Georgiades, *Nature* **362**, 230 (1993).
- [8] A. Schlüter, D. Lortz, and F. H. Busse, *J. Fluid Mech.* **23**, 129 (1965).
- [9] C. W. Gardiner, *Handbook of Stochastic Methods* (Springer-Verlag, New York, 1985).
- [10] M. Seesselberg and F. Petruccione, *Comput. Phys. Commun.* **74**, 303 (1993).
- [11] G. Ahlers, M. C. Cross, P. C. Hohenberg, and S. Safran, *J. Fluid Mech.* **110**, 297 (1981).
- [12] C. M. Meyer, G. Ahlers, and D. S. Cannell, *Phys. Rev. Lett.* **59**, 1577 (1987); *Phys. Rev. A* **44**, 2514 (1991).
- [13] W. Zimmermann (unpublished).
- [14] Y. Pomeau, *J. Phys. (Paris) I* **3**, 365 (1993).
- [15] Hao-wen Xi, J. Viñals, and J. D. Gunton, *Phys. Rev. A* **46**, R4483 (1992).
- [16] H. van Beijeren and E. G. D. Cohen, *J. Stat. Phys.* **53**, 77 (1988); *Phys. Rev. Lett.* **60**, 1208 (1988).